2022

Approximate Calculation Of On-off Vapor Refrigeration Cycle Efficiency Through A Pseudo-stationary Models

Vinicius A. Matsuda

Eduardo Postingel Falcetti

Cristiano Bigonha Tibiriça

Luben Cabezas Gomes

Approximate Calculation Of On-off Vapor Refrigeration Cycle Efficiency Through Pseudo-stationary Models

Vinicius A. MATSUDA [2], Eduardo P. FALCETTI [1,2*], Cristiano B. TIBIRIÇÁ [2], Luben CABEZAS-GÓMEZ [2]

[1]Tecumseh Products Company,
São Carlos, São Paulo, Brazil
eduardo.falcetti@tecumseh.com

[2] Heat Transfer Research Group, Department of Mechanical Engineering, São Carlos School of Engineering, University of São Paulo
São Carlos, São Paulo, Brazil
lubencg@sc.usp.br

* Corresponding Author

ABSTRACT

The present work main objective is the development of a simulation mathematical model for vapor compression refrigeration cycles that can provide approximate average values for the system efficiency, as the coefficient of performance (COP) and the second law efficiency (η_{II}), during on-off operation. For this aim, two different pseudo-stationary models were developed. Each model calculates the cabinet internal air temperature in order to estimate the periods in which the compressor must be tuned on and off, in order to maintain the system in the desired operational regime. The first model considers that the refrigerant pressures in system components, the degrees of sub-cooling and super-heating, the system mass flow-rate and the compressor operational conditions assume constant values, which are equal to the pull-down steady-state simulated values. Otherwise the lumped temperatures of the condenser, evaporator and compressor components and of cabinet air are calculated for each simulated time step. The second model takes into consideration the changes of the compressor operational regime, and thus additionally considers variations in the system mass flow rates. In order to validate the two models, a comparison with available experimental data and various transient simulation data from a detailed transient model was performed. In general, it was observed that both the *COP* and η_{II} presented slightly higher values for the pseudo-stationary models due to consideration of compressor power consumption values calculated for the stationary regime. The *COP* and η_{II} also presented a similar behavior for the variation of the refrigerant charge and environmental temperature in relation to the values obtained with the more detailed simulation model. The developed models can be useful for a quick system analysis, or yet, for a first optimization analysis of the refrigeration system operation.

1.INTRODUCTION

Since its creation, refrigeration systems became indispensable to satisfy human needs in domestic and industrial sectors. The energy consumption of these systems represents roughly 17% of the global energetic consumption, with about 45% of this quantity being due to its domestic use alone IIR (2019). These facts indicate that the optimization of the energetic consumption of these systems became an engineering requirement.

As a first approach in the optimization of complex systems, such as refrigeration cycles, the usage of numerical simulations is a good practice since this kind of analysis often require a lower amount of time when compared with experimental tests and studies. Often numerical simulations address the study of the system transient behavior, allowing a better understanding of the system operation and performance. These simulations can be performed with lumped transient models (Gardenghi, 2020; Gardenghi, Campanini, et al., 2021; Jakobsen, 1995; Matsuda et al., 2022), lumped transient moving boundaries models (McKinley & Alleyne, 2008; Rasmussen & Alleyne, 2006), or yet with discrete transient models (Guzella et al., 2016, 2021).

Although the transient models show good behavior when compared with experimental data and produce comprehensive simulation results of the system performance and operation, the computational effort needed to perform such

simulations tends to be considerable, increasing the time needed to perform such studies.

With these facts in mind, this work address the development of numerical pseudo-stationary models that can compute approximate system average parameters, such as, the compressor electric consumption and the system *COP* and η_{II}. The models can allow the development of quick but reasonable accurate studies of the system performance and its usage as a first simulation approach in system control strategy optimization.

The paper is organized as follows. The methodology, including the derivation of both models along with the adopted simplifying hypotheses, is presented in Sec. 2. The results discussion, including a comparison with experimental results and those numerically obtained with the transient model of Gardenghi, Campanini, et al. (2021) for various compressor rotations and refrigerant charges at the on-off operation, are provided in Sec. 3. Finally the conclusions of the paper are presented in Sec. 4.

2.METHODOLOGY

Two different pseudo-stationary models are proposed in this work. Both models are lumped, but do not account for the calculation of the mass distribution in the system, alike those presented in (Gardenghi, 2020; Gardenghi, Campanini, et al., 2021; Gardenghi, Lacerda, et al., 2021) and Jakobsen (1995). The various model simplifying hypotheses were assumed in order to lower the model dynamics and as a consequence lower the needed computational time.

The first model, called **Model A**, assumes that the refrigerant pressures in system components, the degrees of sub-cooling and super-heating, the system mass flow-rate and the compressor operational conditions are those calculated for the stationary pull-down operation. However, the surface component temperatures (condenser, evaporator and compressor) and the cabinet internal air temperature are considering variable with time, being numerically calculated at each computational time step. These assumptions were considered since it was noted that the pressures, mass flow rates, and temperatures differences (sub-cooling and super-heating) evolve to their respective steady-state values much faster than the component temperatures.

The second model, called **Model B**, additionally includes variations of some system parameters due to the consideration of compressor operational regime. Thus, in this model the variations of the saturation pressures (condensation and evaporation) and consequently of the compressor mass flow and power consumption rates are also taken into account.

In addition, the following simplifying hypothesis were adopted for both models: ***(i)*** control volumes of the system components have only one inlet and one outlet; ***(ii)*** kinetic and potential energies within and at the open boundaries are neglected; ***(iii)*** the thermodynamic and transport properties are uniform in each control volume; ***(iv)*** force fields are neglected; ***(v)***delays in transport, pressure losses and accumulation of refrigerant in the connecting tubes; pressure losses in the condenser and evaporator; spatial temperature variations on the surfaces of the condenser, evaporator and compressor and within the cabinet compartments are all neglected. The simulations do not consider the opening of doors, following the conditions of the experimental tests. Air infiltration is not taken into account.

2.1 Mathematical Model

In this section are described the mathematical models employed for the main system components, namely, compressor, condenser, capillary tube, evaporator and refrigerator cabinet. It is simulated a dual-skin chest-freezer operating with R290. This appliance was studied and simulated in Gardenghi (2020); Gardenghi, Campanini, et al. (2021). All the geometrical characteristics and input models parameters were taken from these two references. It is important to note that both models (A and B) use the stationary results obtained from a pull-down simulation for the saturation pressures P_{cond} and P_{evap} and temperatures degrees ΔT_{SH} and ΔT_{SC}. In this work, this first simulation of system pull-down is realized with a simplified version of the model developed by Gardenghi, Campanini, et al. (2021). These data, however, can be obtained from experiments, for example.

Compressor : The main inputs for this model are: the inlet temperature, T_1, and the evaporation, P_{evap}, and condensation, P_{cond}, pressures. In addition, the following parameters are also necessary: compressor thermal conductance, UA_{com}, compressor thermal capacity, C_{com}, and the compression polytropic exponent, n_p. From all these inputs the following outputs are obtained: the compressor volumetric efficiency, η_{Vol}; the compressor mass flow rate, $\dot{m}_{com}$, the compressor global (isentropic) efficiency, η_{gl}; the compressor consumed power $\dot{W}_{com}$; the compressor wall temperature, T_{com}, and the fluid temperature and enthalpy, T_2 and h_2, respectively, at compressor outlet. Finally, there are other

two inputs variables provided at the beginning of the simulations: the ambient temperature, T_{env}, and the compressor speed, N_{RPM}.

In order to obtain the compressor efficiencies η_{Vol} and η_{gl} curves, the models proposed in Li (2012, 2013), were employed. In addition, UA_{com} was approximately determined from the data available in the manufacturer folders. The coefficients a_n, b_n, $\dot{W}_{loss}$ were determined through the application of the Levenberg-Marquardt method, Levenberg (1944); Marquardt (1963), for the minimization of the least square errors. This method was chosen mainly due to the fact that the minimization process is of the unconstrained type. The equations used for the approximation of the efficiency curves are shown in Tab.1.

Table 1: Compressor Efficiencies.

Volumetric Efficiency (Reference Speed)	$\eta_{Vol_{ref}} = a_1 + a_2 \cdot \left[\frac{P_{cond}}{P_{evap}}\right]^{1/k}$	(1)
Volumetric Efficiency	$\eta_{Vol} = \left[a_3 + a_4 \cdot \left(\frac{N_{RPM}}{N_{RPM_{ref}}}\right) + a_5 \cdot \left(\frac{N_{RPM}}{N_{RPM_{ref}}}\right)^2\right] \cdot \eta_{Vol_{ref}}$	(2)
Isentropic Efficiency (Reference Speed)	$\eta_{gl_{ref}} = \frac{\left\{\dot{V}P_{evap}b_1 \cdot \left[\left(\frac{P_{cond}}{P_{evap}}\right)^{b_2+\frac{k-1}{k}} + \frac{b_3}{P_{cond}}\right] + \dot{W}_{loss}\right\}}{\dot{m}_{com}(h_{2_{isen}} - h_1)}$	(3)
Isentropic Efficiency	$\eta_{gl} = \eta_{gl_{ref}} \cdot \left[b_4 + b_5 \cdot \left(\frac{N_{RPM}}{N_{RPM_{ref}}}\right) + b_6 \cdot \left(\frac{N_{RPM}}{N_{RPM_{ref}}}\right)^2\right]^{-1}$	(4)

The **Model A** works as follows. First, using the pull-down steady-state pull-down values (saturation pressures and temperature degrees) the efficiencies η_{Vol} and η_{gl} are evaluated from Eqs. 2 and 4, respectively. This allows the calculation of the mass flow rate, $\dot{m}_{com}$, through Eq. 5 and of the power consumption, $\dot{W}_{com}$, through Eq.6. In sequence, the compressor discharge temperature, T_2, is evaluated by Eq. 7, and finally, using the known values of P_{cond} and T_2, the condenser inlet state is determined. It is important to remember that these conditions are evaluated at steady-state conditions and are constants in this specific model.

Table 2: Equations for the compressor sub-model.

Mass flow rate	$\dot{m}_{com} = \eta_{vol}\rho_1\dot{V}_{disp}\frac{N_{RPM}}{60}$	(5)
Electric power consumption	$\dot{W}_{com} = \dot{m}_{com}\frac{(h_{2s} - h_{1,std})}{\eta_{gl}}$	(6)
Discharge temperature	$T_2 = \left(\frac{T_1 + T_{com}}{2}\right)\left(\frac{P_{cond}}{P_{evap}}\right)^{\frac{n_p-1}{n_p}}$	(7)
Heat transfer rate through the housing	$\dot{Q}_{com} = UA_{com}(T_{com} - T_{env})$	(8)
Housing temperature	$C_{com}\frac{dT_{com}}{dt} = \dot{W}_{com} - \dot{Q}_{com} + \dot{m}_{com} \cdot (h_{1,std} - h_{2,std})$	(9)

In the **Model B** the compressor efficiencies are computed for each cycle (denoted by one integration time step). This fact implies that P_{cond} and P_{evap} variations are also considered along the simulations using their input values equal to those calculated for the pull-down steady-state operation. These pressure values for each cycle are estimated through the saturation temperatures calculated in the condenser and evaporator sub-models. This procedure leads to a compressor efficiencies variation, and as a consequence, to a variation of m_{com} and W_{com} at each time step, resulting in evaluation of new compressor surface temperature, T_{com}, trough Eq. 9. It should be noted that in this model only the compressor parameters vary, and the other component thermodynamic states remain constant and equal to the states calculated for the pull-down steady-state.

Condenser : The inputs parameters of this model are: the outlet state of the compressor, defined by h_2 and T_2; the compressor mass flow rate, $\dot{m}_{com}$; the condensation pressure; and the sub-cooling degree, ΔT_{SC}. Additionally, some experimental inputs are needed: the condenser thermal conductance and capacity, UA_C and C_C, all determined in

Gardenghi, Campanini, et al. (2021). The model gives the following outputs variables: the fluid outlet temperature and enthalpy, T_3 and h_3; the condenser external heat transfer rate, $\dot{Q}_{C,ext}$; the condenser internal heat transfer rate, $\dot{Q}_{C,int}$, and the condenser surface temperature, T_{wc}.

Table 3: Equations for the condenser sub-model.

External heat transfer rate	$\dot{Q}_{C,ext} = UA_C \cdot [T_{env} - T_{wc}]$	(10)
Internal heat transfer rate	$\dot{Q}_{C,int} = \dot{m}_{com} \cdot (h_{2,std} - h_{3,std})$	(11)
Condenser Temperature Derivative	$\frac{dT_{wc}}{dt} = \frac{\dot{Q}_{C,ext} + \dot{Q}_{C,int}}{C_C}$	(12)
Condensation Temperature	$T_{cond} = T_{wc} + \frac{\dot{Q}_{C,int}}{\overline{h}_{cond} A_{ci}}$	(13)
Heat Transfer Coefficient	$\overline{h}_{cond} = \frac{\dot{m}_{com,std} \cdot (h_{2,std} - h_{3,std})}{A_{ci}(T_{cond,std} - T_{wc,std})}$	(14)

For **Model A**, the condenser internal heat transfer rate is assumed to be constant and is calculate at the pull-down steady state conditions. The condenser surface temperature is calculated through Eq. 12 in each time step. Since **Model B** accounts for the change in the compressor operation regime, the condensation temperature must be evaluated, this can be done in a similar way as done in the thermal model developed by Gardenghi (2020); Gardenghi, Campanini, et al. (2021), resulting in Eq. 13, h_{cond} stands for the average heat-transfer coefficient estimated trough the pull-down conditions, as in Eq. 14. Its important to note that for **Model B**, Eq. 11, is estimated at each time step, with the corresponding enthalpy and mass flow rates.

Capillary Tube : The model used for the capillary tube is the same for both **Model A** and **Model B**, the capillary tube is assumed to be adiabatic, causing an isenthalpic expansion process. The system takes as its inputs both the enthalpy at the condenser outlet(h_3) and the evaporation pressure, and returns the state of the capillary tube outlet, defined by both the evaporation pressure and the enthalpy at the condenser outlet.

Evaporator : The inputs parameters of this model are: the outlet state of the capillary tube, defined by h_4 and P_{evap}; the compressor mass flow rate, $\dot{m}_{com}$; and the super-heating degree, ΔT_{SH}, the evaporator thermal conductance and capacity, UA_E and C_E, experimentally determined in Gardenghi, Campanini, et al. (2021). The model gives the following outputs variables: the fluid outlet temperature and enthalpy, T_1 and h_1; the evaporator external heat transfer rate, $\dot{Q}_{E,ext}$; the evaporator internal heat transfer rate, $\dot{Q}_{E,int}$, and the evaporator surface temperature, T_{we}.

Table 4: Equations for the evaporator sub-model.

External heat transfer rate	$\dot{Q}_{E,ext} = UA_E \cdot [T_{cab} - T_{we}]$	(15)
Internal heat transfer rate	$\dot{Q}_{E,int} = \dot{m}_{com} \cdot (h_{4,std} - h_{1,std})$	(16)
Evaporator Temperature Derivative	$\frac{dT_{we}}{dt} = \frac{\dot{Q}_{E,ext} + \dot{Q}_{E,int}}{C_E}$	(17)
Evaporation Temperature	$T_{evap} = T_{we} + \frac{\dot{Q}_{E,int}}{\overline{h}_{evap} A_{ei}}$	(18)
Heat Transfer Coefficient	$\overline{h}_{evap} = \frac{\dot{m}_{com,std} \cdot (h_{4,std} - h_{1,std})}{A_{ei}(T_{evap,std} - T_{we,std})}$	(19)

For **Model A**, the evaporator internal heat transfer rate is assumed to be constant and is calculate at the pull-down steady state conditions. The evaporator surface temperature is calculated through Eq. 17 at each time step. Since **Model B** accounts for the change in the compressor operation regime, the evaporation temperature must be evaluated. This can be realized as performed for the thermal model developed by Gardenghi (2020); Gardenghi, Campanini, et al. (2021), resulting in Eq. 18. h_{evap} stands for the average heat-transfer coefficient, which is estimated trough the pull-down conditions, by Eq. 19. It is important to note that for **Model B**, Eq. 16, is estimated at each time step, with the corresponding enthalpy and mass flow rate values.

Cabinet : The inputs for this model are: the evaporator wall temperature, T_{we}, the external heat transfer rate in the evaporator, $\dot{Q}_{E,ext}$, the cabinet conductance and thermal capacity, UA_{cab} and C_{cab}, experimentally determined. The

outputs of the model are the temperature of the air inside cabinet, T_{cab}. First the heat transferred to the cabinet from the ambient is computed by Eq. 20. Then, applying an energy conservation on the cabinet control volume the cabinet temperature time derivative, given by Eq. 21, is obtained. Integrating this equation T_{cab} is calculated. For the cabinet sub-model there is no difference between **Model A** and **Model B**.

Table 5: Equations for the cabinet thermal sub-model.

Heat transfer rate through the walls	$\dot{Q}_{cab} = UA_{cab} \cdot (T_{env} - T_{cab})$	(20)
Temperature inside freezer	$\frac{dT_{cab}}{dt} = \frac{\dot{Q}_{cab} + \dot{Q}_E}{C_{cab}}$	(21)

2.2 Second Law Analysis

The Second Law Efficiency (SLE) can be defined as the relation between the maximum achievable coefficient of performance, COP_{rev}, and the real system COP. Mathematically COP_{rev} can calculated as a function of the reversible power received by the system, $\dot{W}_{rev}$, and the exergy destroyed in the system, according to Eq. 22. The reversible power is given by Eq. 23.

$$\eta_{II} = \frac{COP}{COP_{rev}} = \frac{\dot{W}_{rev}}{\dot{W}_{rev} + \dot{X}_{des,sys}} \tag{22}$$

$$\dot{W}_{rev} = \left[1 - \frac{T_{cab}}{T_{env}}\right] \dot{Q}_E \tag{23}$$

In order to estimate the average SLE for the system, the total rate of exergy destroyed in the system must be calculated. Taking into account that exergy is an additive property, Eq. 24 can be written. In this equation the individual contributions of each subsystem can be calculated through the equations presented in Table 6. The internal energy derivatives, $\frac{dU}{dt}$, can be estimated through the energy conservation equations for the respective sub-model, Eq. 9 for the compressor, Eq. 12 for the condenser and Eq. 17 for the evaporator, respectively. Its important to remind that ($\frac{dU_{com}}{dt}$) will only be calculated for **Model B**.

$$\dot{X}_{des,sys} = \dot{X}_{des,com} + \dot{X}_{des,C} + \dot{X}_{des,cap} + \dot{X}_{des,E} \tag{24}$$

Table 6: Equations for the Exergy Destruction Rates.

Compressor Exergy Destruction Rate	$\dot{X}_{des,com} = \dot{W_{com}} + \dot{m}_{com} \cdot \left[\left(h_{1,std} - h_{2,std}\right) + T_{env} \cdot \left(s_{2,std} - s_{1,std}\right)\right] - \frac{d}{dt} U_{com} \cdot \left(1 - \frac{T_{env}}{T_{com}}\right)$	(25)
Condenser Exergy Destruction Rate	$\dot{X}_{des,C} = \dot{m}_{com} \cdot \left[\left(h_{2,std} - h_{3,std}\right) + T_{env} \cdot \left(s_{3,std} - s_{2,std}\right)\right] - \frac{d}{dt} U_C \cdot \left(1 - \frac{T_{env}}{T_{wc}}\right)$	(26)
Capillary Tube Exergy Destruction Rate	$\dot{X}_{des,cap} = \dot{m}_{com} \cdot T_{env} \cdot \left[s_{4,std} - s_{3,std}\right]$	(27)
Evaporator Exergy Destruction Rate	$\dot{X}_{des,E} = \dot{m}_{com} \cdot \left[\left(h_{4,std} - h_{1,std}\right) + T_{env} \cdot \left(s_{1,std} - s_{4,std}\right)\right] - \frac{d}{dt} U_E \cdot \left(1 - \frac{T_{env}}{T_{we}}\right)$	(28)

3.RESULTS

In this section the simulation results obtained with both models are shown. The results include the values of: average system efficiencies, COP_{avg} and $\eta_{II,avg}$; compressor monthly energy consumption; average compressor consumption, $\dot{W}_{com,avg}$; and the average cooling capacity, $\dot{Q}_{e,avg}$. These simulated results are analyzed both graphically and through the root mean square (RMS) errors in relation to the values obtained with the transient model developed by Matsuda et al. (2022), extensively validated against experimental data, and called **Transient model**.

All the simulations were performed for 1200min of operation for environmental temperature equal to T_{env} = 25° and various refrigerant charge values. The temperature limits for the on-off control were set to $-19.5°C$ and $-22.3°C$, as the upper and lower temperatures, respectively. In general **Model A** needs about 1min47s to perform each simulation while **Model B** needs about 13min10s, its important to note that this values are for the pseudo-stationary models alone, not including the time spent for the pull-down simulation to acquire the steady-state condition for the given refrigerant mass.

First, its interesting to compare the results obtained for both models with experimental results, that were obtained for the refrigerant charge of 103g and a compressor rotation of 4500 RPM with the temperature conditions show above. The results are shown in Tab. 7 and comprehend the COP_{avg}, the monthly energy consumption, $\dot{W}_{com,avg}$ and $\dot{Q}_{e,avg}$ for the experimental tests, for the Transient model and the pseudo-stationary models. As expected the values achieved for the COP_{avg} are slightly higher for the pseudo-stationary models. These results can be associated with the simplifications used for the both models. In both cases the pull-down steady state is used to estimate the stationary system performance. With this simplification the more unstable part of the operation regime are neglected and the compressor presents a lower average power consumption, resulting in a over estimation of system COP.

Table 7: Average performance parameters obtained by simulations and experimental tests in the *On-Off* operation.

	COP $[W/W]$	Monthly Consumption $[kWh\ \text{month}^{-1}]$	$\dot{W}_{com,avg}$ $[W]$	$\dot{Q}_{e,avg}$ $[W]$
Experimental	0.65 ± 0.05	222.50 ± 3.34	309.03 ± 4.64	201.01 ± 14.34
Transient Model	0.63	217.92	302.67	189.33
Model A	0.67	204.84	284.50	198.69
Model B	0.72	204.43	283.93	203.99

In Figure 1 are shown the results for a constant refrigerant charge of 200g simulated with different compressor rotation speeds. In these conditions the tendency of all studied parameters shown a good agreement in relation with the ones presented by the Transient model. The results show a decay of COP and η_{II} with the increase of the compressor rotation. In special **Model A** presented a closer values for the COP_{avg}, $\dot{W}_{com,avg}$ and consequently the estimated monthly consumption in relation to the transient model, which translates to the lowers errors, RMS_{error}, shown in Tab.8.

Table 8: Efficiency Parameters RMS_{error} for 200g.

	COP $[\%]$	η_{II} $[\%]$	Consumption $[\%]$	$\dot{W}_{com,avg}$ $[\%]$	$\dot{Q}_{e,avg}$ $[\%]$
Model A	7.12	24.55	0.87	0.87	6.59
Model B	14.67	13.09	8.49	8.49	5.06

As can be seen in Fig. 1, the values simulated for an specific efficiency parameter become worse with the increase of the compressor rotation speed. With this in mind, simulations with various refrigerant charges were performed with a compressor rotation of 4500/RPM. The results are shown in Fig. 2. As can be noted, the achieved results for both models predict the behavior of the analyzed parameters for the various refrigerant charges with relative satisfactory RMS errors. Overall, the **Model A** presented lower RMS error values than **Model B**, despite its higher simplicity. The values of the obtained RMS errors are shown in Table 9. The higher RMS errors where obtained for average COP_{avg} and $\eta_{II,avg}$.

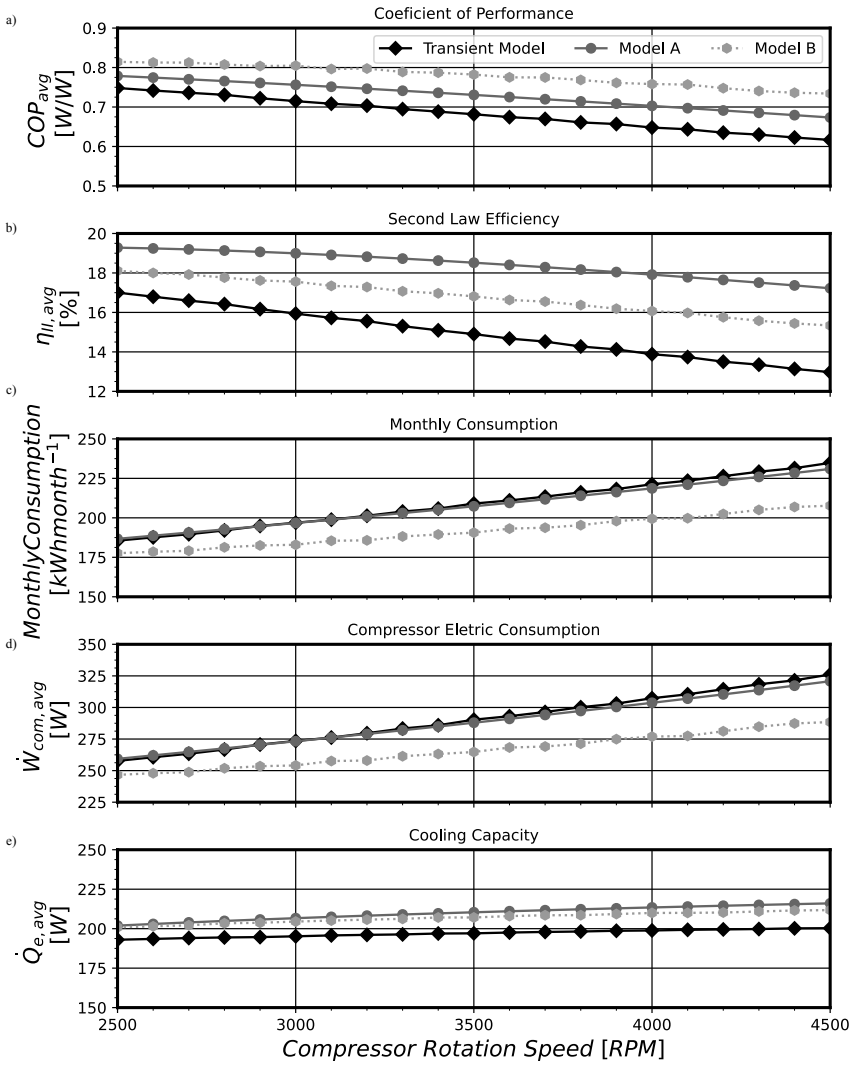

Figure 1: Results Obtained for a refrigerant charge of 200g for various compressor rotations. a) Coefficient of Performance; b) Second Law Efficiency; c) Average Monthly Consumption; d) Average Compressor Consumption; e) Average Cooling Capacity.

Table 9: Efficiency Parameters RMS errors for 4500RPM.

	COP [%]	η_{II} [%]	Consumption [%]	$\dot{W}_{com,avg}$ [%]	$\dot{Q}_{e,avg}$ [%]
Model A	6.35	10.11	9.86	9.86	4.13
Model B	16.62	15.18	9.68	9.68	5.60

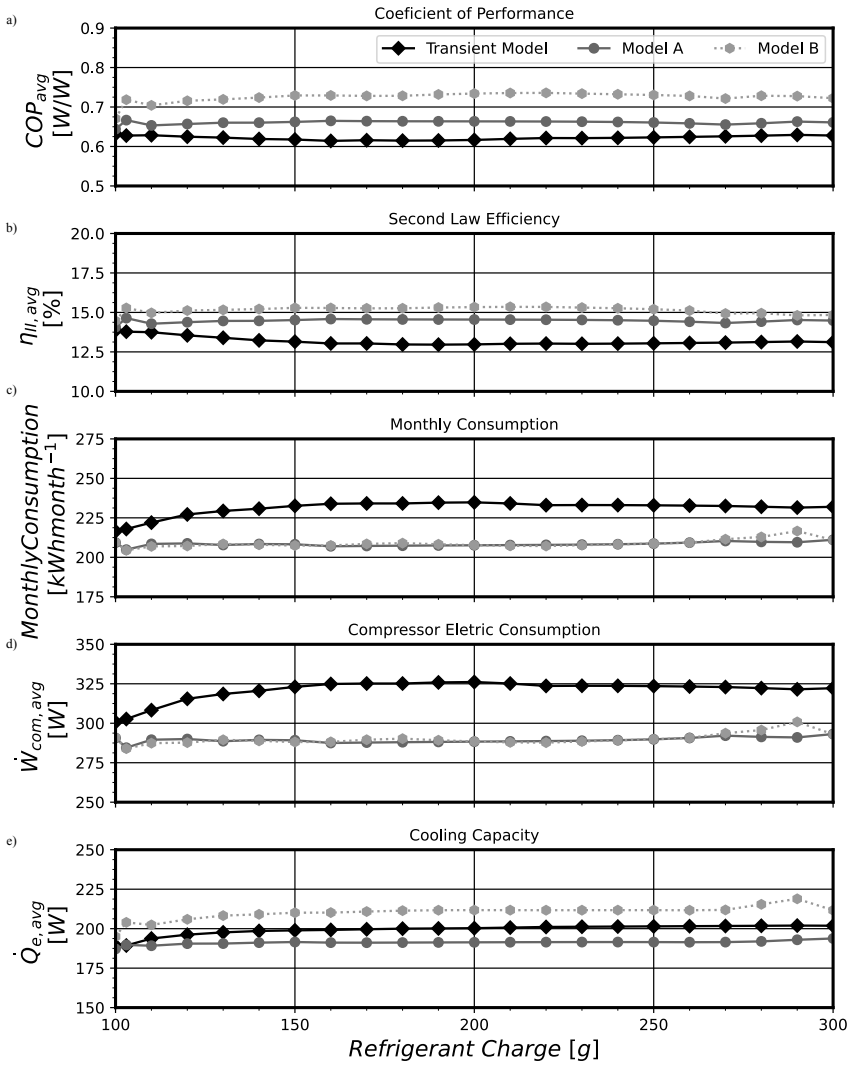

Figure 2: Results obtained for 4500*RPM* for various refrigerant charges. a) Coefficient of Performance; b) Second Law Efficiency; c) Average Monthly Consumption; d) Average Compressor Consumption; e) Average Cooling Capacity.

4.CONCLUSION

In this work to pseudo-stationary models were developed and tested against the transient capacitive model developed in Gardenghi (2020); Gardenghi, Campanini, et al. (2021). In general both models showed close values for the average system efficiencies, COP_{avg} and $\eta_{II,avg}$; compressor monthly energy consumption; average compressor consumption, $\dot{W}_{com,avg}$; and the average cooling capacity, $\dot{Q}_{e,avg}$, serving as a first tool for the study and optimization of Vapor Compression Refrigeration Systems. Despite the good results achieved when comparing singular values, both models failed to predict an accurate behavior for the efficiencies parameters when the tests were performed with refrigerant charges at a constant compressor speed. When analyzing the results for a constant refrigerant charge and various N_{RPM}, both models were capable of predicting the behavior of the studied efficiencies parameters. Finally **Model A** presented lower RMS_{error} than **Model B**, despite its higher simplicity, which along its lower required computational effort makes this model a better tool for a preliminary analysis of the system when compared with **Model B**.

NOMENCLATURE

C	thermal capacitance	(W/K)
N_{RPM}	compressor rotation	(rpm)
P	pressure	(Pa)
T	temperature	(K)
UA	thermal conductance	(W/K)
$\dot{m}$	mass flow rate	(kg/s)
$\dot{Q}$	power	(W)
$\dot{W}$	power	(W)
$\forall$	volume	(m^3)
η	efficiency	$(-)$

Subscript

cab	cabinet
com	compressor
cond	condensation
evap	evaporation
ext	external
gl	global
int	internal
SC	sub-cooling
SH	super-heating
std	pull-down steady-state
Vol	volumetric
wc	condenser surface
we	evaporator surface
II	second law
2*s*	isentropic state 2

REFERENCES

Gardenghi, Á. R. (2020). *Transient modeling of vapor compression refrigeration systems for domestic applications*. Masters dissertation, Mechanical Engineering Department - São Carlos School of Engineering, University of São Paulo, São Carlos, Brazil.

Gardenghi, Á. R., Campanini, M. M., Lacerda, J. F., Tibiriçá, C. B., & Cabezas-Gómez, L. (2021). A detailed study of the transient behavior of dual-skin chest-freezer with r290. *International Journal of Refrigeration*, *131*, 300–311.

Gardenghi, Á. R., Lacerda, J. F., Tibiriçá, C. B., & Cabezas-Gómez, L. (2021). Numerical and experimental study of the transient behavior of a domestic vapor compression refrigeration system–influence of refrigerant charge and ambient temperature. *Applied Thermal Engineering*, *190*, 116728.

Guzella, M. d. S., Cabezas-Gómez, L., da Silva, J. A., Maia, C. B., & Hanriot, S. d. M. (2016). Numerical modeling of the thermal–hydraulic behavior of wire-on-tube condensers operating with hfc-134a using homogeneous equilibrium model: evaluation of some void fraction correlations. *Heat and Mass Transfer*, *52*(2), 183–195.

Guzella, M. d. S., Cabezas-Gómez, L., & Guimarães, L. G. M. (2021). Numerical simulation of a single-compartment household refrigerator during start-up transient and stationary cyclic operation with different refrigerant charges. *Arabian Journal for Science and Engineering*, *46*(8), 7533–7542.

IIR. (2019). *The role of refrigeration in the global economy*. 38th Informatory Note on Refrigeration Technologies/November 2019.

Jakobsen, A. (1995). Energy optimization of refrigeration systems. *Doctoral thesis, Technical University of Denmark (DTU)*.

Levenberg, K. (1944). A method for the solution of certain non-linear problems in least squares. *Quarterly of Applied Mathematics*, *2*(2), 164–168.

Li, W. (2012). Simplified steady-state modeling for hermetic compressors with focus on extrapolation. *International journal of refrigeration*, *35*(6), 1722–1733.

Li, W. (2013). Simplified steady-state modeling for variable speed compressor. *Applied thermal engineering*, *50*(1), 318–326.

Marquardt, D. W. (1963). An algorithm for least-squares estimation of nonlinear parameters. *Journal of the Society for Industrial and Applied Mathematics*, *11*(2), 431-441.

Matsuda, V. A., Gardenghi, Á. R., Tibiriçá, C. B., & Cabezas-Gómez, L. (2022). Thermodynamic irreversibility analysis of dual-skin chest-freezer. *Entropy*, *24*(4), 453.

McKinley, T. L., & Alleyne, A. G. (2008). An advanced nonlinear switched heat exchanger model for vapor compression cycles using the moving-boundary method. *International Journal of refrigeration*, *31*(7), 1253–1264.

Rasmussen, B. P., & Alleyne, A. G. (2006). *Dynamic modeling and advanced control of air conditioning and refrigeration systems* (Tech. Rep.). Air Conditioning and Refrigeration Center. College of Engineering.

ACKNOWLEDGMENT

The first author acknowledges the scholarship (PIBIC) received from National Council for Scientific and Technological Development (CNPq) - Brazil. The authors acknowledge the support received from Tecumseh do Brasil LTDA for paper presentation. The support received from FAPESP (São Paulo Foundation for Research Support, process 2016/09509-1) for running numerical simulations is also acknowledged.